

# MODELING OF RAYLEIGH-TAYLOR INSTABILITY FOR STEAM DIRECT CONTACT CONDENSATION

**M. Pellegrini, M. Naitoh**

The Institute of Applied Energy, Nuclear Power Engineering Center Shimbashi  
SY Bldg. 1-14-2 Nishi-Shimbashi, Minato-ku, Tokyo, 105-0003 Japan  
mpellegrini@iae.or.jp; mnaito@iae.or.jp

**C. Josey, E. Baglietto**

Department of Nuclear Engineering  
Massachusetts Institute of Technology, Nuclear and Science Engineering  
77 Massachusetts Avenue, 24-107 Cambridge, MA 02139 USA  
emiliob@mit.edu

## ABSTRACT

Passive systems are commonly employed in nuclear reactors to enhance safety during postulated accidents. However these systems, such as direct contact condensation, might introduce complex and unexpected phenomena, possibly reducing the efficiency in case of long transients. A similar event is expected during the Fukushima Daiichi accident in the suppression pool, where the reduction in steam condensation might have resulted in local steam by-pass increasing the containment pressure. Detailed analyses of such complex phenomena are therefore necessary and various attempts have been performed in the past to develop related two-phase two-fluid Computational Fluid Dynamics (CFD) models. The most successful CFD investigations of the related phenomena focused on the definition of a heat transfer coefficient from the water side, based on the surface renewal theory and the turbulent scales. Little effort was however attempted to add a general model of the interfacial area based on theoretical and experimental evidences. In the present work it is proposed a method to treat the surface with growing instabilities based on the Rayleigh-Taylor theory, leading to the break-up of the surface and triggering steam depressurization typical of chugging phenomena. The preliminary results of the implemented technique have demonstrated the capability to predict the characteristic phases of chugging (bubble collapse, depressurization and steam flow upward in the pipe) with a considerable improvement in the prediction compared to previous investigations. The result assumes remarkable interest in the perspective of the employment of multiphase CFD for the prediction of the water temperature distribution within the suppression pool since the presence of chugging introduces large water mixing at the onset of every water discharge cycle.

## KEYWORDS

Direct contact condensation, two-phase flow, CFD, Rayleigh-Taylor instability, interfacial area

## 1. INTRODUCTION

Steam Direct Contact Condensation (DCC) is a well-known method to condense steam, which has been widely employed in the industry (e.g. nuclear, marine and chemical) for its high efficiency and ease of implementation due to the relatively simple design. In the nuclear field such philosophy has been introduced in the design of safe nuclear power plants, mostly because DCC serves as a passive safety system in case of a postulated accident. On the other hand, DCC might create unstable configurations of the flow, resulting in rapid pressure transients and large flow recirculation within the water pool, which could harm the plant structure integrity and reduce the efficiency of the whole system.

For the study of DCC, experiments have been performed since the early '70s. The most well-known experiments resulted in the development of regime maps for different macroscopic phenomena of the condensation (refer to [1], [2], [3], [4], [5]). The comprehensive work in [6] summed up the available experimental data presenting the DCC in three macro regions, chugging, bubbling and jetting based on three dependencies, pipe diameter, steam mass flux and pool water subcooling. The chugging regime has been probably the one that has attracted the largest attention in the nuclear field. The reason is that, dealing with violent condensation associated to a quick pressure ramp in the steam flow and water pool, it results in large loads on the pool structures. Chugging is characterized by steam ejected through a relatively large pipe diameter, at low steam mass flux and large subcooling. Such conditions have been observed during steam blowdown in the postulated event of a design basis Loss of Coolant Accident (LOCA).

The first theoretical studies approached the chugging modeling for the description of the pressure oscillations in the system. Sargis et al. [7] presented an interesting model based on the conservation laws to predict pressure transient during the steam chugging. In their approach the bubble is assumed to be hemispherical and the condensation mass flux follows the kinetic theory assuming the interface temperature. With the developed method they were able to predict the pressure transients with a qualitative good agreement against the observations. Nariai and Aya [8] propose a linear frequency analysis to investigate the oscillation frequency. The model has been developed assuming cylindrical, spherical and hemispherical bubble shape. Applying a value of the heat transfer coefficient, following the approach of the same authors, realistic frequency values were obtained.

More recently analytical two-phase flow Computational Fluid Dynamics (CFD) applications have also been developed [9], in particular as validation of the POOLEX series of experiment [10]. Tanskanen develops a two-phase Eulerian-Eulerian modeling in [9, 11] interpreting the chugging phenomenon as in the theoretical analyses introduced above. In other words the steam bubble, discharged into the water pool, develops a large level of turbulence which increases the heat transfer locally, causing the subsequent large depressurization. In their model the heat transfer coefficient has been derived based on separated (or stratified) flow analyses such as surface renewal [12] or surface convergence [12]. Results have presented a general agreement in the global phenomenon, with flow pressure variations that were in a qualitative agreement with the experimental values [11]. However, as presented in [12] the approach fails to be general for cases with different conditions and the prediction of the water-steam interface moving within the pipe appears different from recent observations [14]. Also, the phenomenology of the bubble implosion appears different from what observed in the experiment.

At the best of authors' knowledge, a detailed investigation of the bubble surface area has not been taken into consideration in the studies available until today. The area, expressed as area density, has been defined either as Sauter mean diameter or as volume fraction gradient [11]. In the present investigation we add, to the computation of the interfacial area, the amplification effect of destabilization of the surface, which has been modeled in our preliminary approach following the concepts of the Rayleigh-Taylor instability (RTI) [15]. The RTI is usually created at the interface of a fluid sitting on the top of one with lower density immersed in a gravitational field, whose interface develops exponentially increasing wave amplitudes [16, 17]. In more general terms the RTI appears when a high-density fluid is accelerated in the direction of a low-density fluid. We intend the steam bubble during a chugging implosion in such configuration, once the pressure inside the bubble is reduced below the pressure of the surrounding liquid.

In the following, the first attempt to implement the above idealization of the problem will be presented and application to the POOLEX STB-24, as in the case of [11], will demonstrate the large potential of the approach, strengthening the necessity to introduce a model which accounts for the surface instability for a correct phenomenological characterization of the chugging phenomenon.

## 2. EULERIAN-EULERIAN CONDENSATION MODELING

Two-fluid Eulerian-Eulerian solution for two-phase flow has been chosen as the method for the solution of the steam DCC. Surface tracking methods (e.g. VOF) appear also suitable for our purposes but, requiring a larger mesh points for the solution of the fine interface, in particular during the implosion, will reduce the study to few implosions. On the other hand, our primary interest is the application of the present approach to real-scale applications.

The two fluid equations and models are solved employing the commercial CFD software STAR-CCM+ 9.06.007 [18]. The two fluid equations are derived from the single phase flow, averaging in space and time across the interface in order to obtain a single set of equations for the two fluids which can reproduce the conditions of the gas, liquid and interphase. Such derivation is presented in [19].

The continuity equation is expressed as

$$\frac{\partial}{\partial t}(\alpha_i \rho_i) + \nabla \cdot (\alpha_i \rho_i \mathbf{v}_i) = \sum_{i \neq j} (\dot{m}_{ij} - \dot{m}_{ji}) \quad (1)$$

where the relation  $\sum_i \alpha_i = 1$  holds.  $\dot{m}_{ij}$  and  $\dot{m}_{ji}$  represent the mass transfer between phase i and j during steam condensation or water evaporation. Such quantities are calculated through closure models and coupled with momentum and energy source terms. The momentum equation requires the definition of the drag components. The effect of drag might influence the bubble shape and the creation of turbulence in the surrounding of the interface but it is considered secondary in our application and therefore not discussed in detail within the present paper. The energy equation and the required closure terms play instead a critical role on the final predictions and need to be addressed in detail. The energy equation reads

$$\begin{aligned} \frac{\partial}{\partial t}(\alpha_i \rho_i E_i) + \nabla \cdot [\alpha_i \rho_i H_i] (\mathbf{v}_i - \mathbf{v}_g) + \nabla \cdot \alpha_i \mathbf{v}_g p = \\ \nabla \cdot (\alpha_i k_{eff,i} \nabla T_i) + \nabla \cdot (T_i \cdot \mathbf{v}_i + \boldsymbol{\tau}_i^t) + \mathbf{f}_i \cdot \mathbf{v}_i + \sum_{i \neq j} Q_i^{ij} + \sum_{i \neq j} (\dot{m}_{ij} - \dot{m}_{ji}) h_i(T_{ij}) \end{aligned} \quad (2)$$

where our interest is concentrated on the last two summations where  $Q_i^{ij}$  and  $Q_j^{ji}$  represent the volumetric heat transferred between the two phases,  $h_i$  the enthalpy associated to the mass transfer  $\dot{m}_{ij} - \dot{m}_{ji}$ . The closure relations for the condensation terms need to be modeled. Water is solved as an incompressible fluid with density set at the value correspondent to the initial water temperature. On the other hand, a crucial point of the DCC regime, in particular during chugging, is accounting for the compressibility of steam. Steam is treated as a compressible gas with density dependent on pressure and temperature. In order to obtain stable solutions the steam density decrease was limited up to around 30 kPa below the atmospheric pressure. This value was chosen based on typical pressure variations during the experiments.

The calculation is carried out in unsteady state with constant time step equal to 5e-4 s, maintaining a Courant number below 1. The convergence criteria adopted to move to the subsequent time step was defined so that in 20 iterations the interfacial mass transfer difference would be lower than 0.001 kg/s, which is roughly 1% of the inlet steam mass flow rate.

## 2.1. Closure Relations

The volumetric heat transfer among phases reads

$$Q_i^{jj} = h_i^{jj} a_{ij} (T_{ij} - T_i) \quad (3)$$

where  $T_i$  is the  $i$  phase temperature and  $T_{ij}$  represents the saturation temperature. Two additional models are required for the definition of the heat transfer coefficient  $h_i^{jj}$  and the interfacial area density,  $a_{ij}$  in order to close the system.

### 2.1.1. Heat transfer coefficient

The heat transfer coefficient is usually expressed in a non-dimensional form such as  $Nu = a Re^b Pr^c$ . In the present application the correlation by Hughes and Duffey in [12] and presented in eq. (4) has been employed because this relation has a general theoretical basis coherent for our purposes. The equation indeed is based on the assumption that the amount of heat transferred depends on the renewal period of a fresh element close to the interface. Their correlation in non-dimensional form reads

$$Nu_L = \frac{2}{\sqrt{\pi}} Re_t^{1/2} Pr^{1/2} \quad (4)$$

$$Re_t = \frac{u_t l_t}{\nu} \quad (5)$$

It should be noticed that the exponent of the turbulent Reynolds number in eq. (4) is instead quite different from the value employed in [9, 11]. In their analysis the exponent is equal to 1, which largely affects the behavior of the condensation. It is worth mentioning also that other reliable correlations exist for the Nusselt number which has not been employed in the present work. Future analysis might consider the sensitivity of the results based on this parameter. The expression of the Nusselt number proposed by Hughes and Duffey is general and its value depends on the choice of the values chosen for the velocity,  $u_t$ , and length,  $l_t$ , scales to be adopted. We follow the approach of [9] which is describing the two scales following the  $k$ - $\varepsilon$  turbulent model

$$l_t = C_\mu^{3/4} \frac{k^{3/2}}{\varepsilon} \quad u_t = C_\mu^{1/4} k^{1/2} \quad (6)$$

In the present work the standard  $k$ - $\varepsilon$  model is adopted to describe the length scales as in equation (6) and to maintain a reasonable number of equations, so that Reynolds stress models are not considered. Wall functions are used for the solution at the first cell on the wall maintaining suitable  $y^+$  in the nominal conditions of the steam flow rate.

### 2.1.2. Interfacial area density

In case of the application of the two-fluid model to a dispersed flow (i.e. when the real interface is smaller than the computational cell) the calculation of the interfacial area is usually addressed following the

concept of the Sauter mean diameter, where a length scale, representing the average bubble diameter, needs to be defined.

In case, as in the present application, where the main interface is larger than the computational cell the gradient of the steam volume fraction guarantees the minimum surface area averaged among several cells, as reported in (7) and adopted in [9, 11].

$$a_{ij} = |\nabla \alpha_s| \quad (7)$$

To demonstrate its applicability, we refer to the example presented in Figure 1 a).

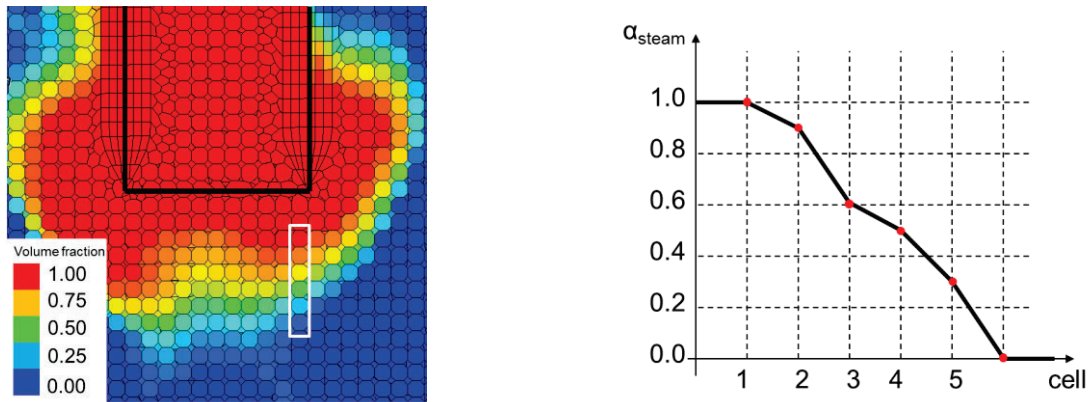


**Figure 1 a) qualitative bubble volume fraction b) volume fraction variation on a generic line presented in a).**

If we assume that the mesh elements in the region marked with the white box in Figure 1 are equal cubes of length  $l$ , the value of the interfacial area associated to the region should be  $l^2$ . The volumetric integral of the area density on the cells marked with the white box in Figure 1 a) and presented in the plot of Fig. 1 b) reads

$$S = \frac{0.1}{l} l^3 + \frac{0.3}{l} l^3 + \frac{0.1}{l} l^3 + \frac{0.2}{l} l^3 + \frac{0.3}{l} l^3 = l^2 \quad (8)$$

From the above equation is immediate the extension of definition of the interfacial area density to the whole domain which provides the minimum surface of the bubble.

### 2.1.3. Rayleigh-Taylor instability introduction

The interfacial area density as described above is the expression of the large scale interface, however it does not account for surface variation which are smaller than the computational cell and that can be created in the flow because of the unstable configuration reached by the steam bubble. The following method, which represents essentially the new insight brought up by the present analysis, attempts to add the effect of the amplified interfacial area modeling the RTI. The following model development is based on the investigation done by Josey in [15] with several modifications for the application to our case.

In general the RTI is created when a high density fluid is located above a lower density fluid and immersed in a gravitation field. The wave amplitude can be expressed as

$$\frac{d\eta}{dt} = n\eta \quad (9)$$

$$n = f(g, k, A) \quad (10)$$

$$A = \frac{\rho_w - \rho_v}{\rho_w + \rho_v} \quad (11)$$

where  $\eta$  is the wave amplitude and  $n$  is a function, to be determined, of gravity, wave number ( $k$ ) and the Atwood number ( $A$ ). The  $n$  function, derived by the simplest theories for interface instability, is expressed as  $n = \sqrt{Agk}$  which is not satisfactory for explaining most of the observations [16]. Duff et. al [16] adds the effect of viscosity and diffusion to the formulation which presented a better agreement with the amplitude of several experiments. His final result is presented in eq. (12) however without the diffusion effect because in the case of condensation, at the interface, the gradient is effectively infinite implying a null diffusion coefficient.

$$n = \sqrt{Agk + \nu^2 k^4 - \nu k^2} \quad (12)$$

A critical component that was missing in the Duff analysis, because apparently negligible in the experiments he analyzed, is the effect of the surface tension. Livescu presented an investigation that takes into account the surface tension and more [17]. Livescu added terms including surface canceling effects and compressibility. For our purposes we consider that the surface tension plays a major role and, to avoid complications and transcendental equations, only this term is considered. The expression derived by Livescu for the  $n$  function reads

$$n = \sqrt{\left( Ag - \frac{\sigma k^2}{\rho_w + \rho_s} \right) k} \quad (13)$$

where  $\sigma$  is the surface tension. An obvious comparison can be done between Eq. (12) and Eq. (13) so that, if the two equations were combined, we would obtain a function for  $n$  that reads

$$n = \Re \left( \sqrt{\sqrt{\left( Ag - \frac{\sigma k^2}{\rho_w + \rho_s} \right) k} + \nu^2 k^4 - \nu k^2} \right) \quad (14)$$

where  $\Re$  indicates that we are interested only in the real component. The approach adopted for the combination of the equations (12) and (13) is the same Duff used to combine the viscosity and diffusion terms together [16], stating that such approach had the effect to neglect the cross-terms, which are assumed in this work to be close to zero. In Eq. (14) we have all the physics included and a relatively easy to handle, algebraic and non-transcendental equation which could be implemented in STAR-CCM+ by the simple employment of user field functions.

## 2.2. Implementation in STAR-CCM+

The implementation in the CFD code requires a certain amount of simplifications and assumptions in order to allow the computations and reach a proper convergence, in particular during the bubble crash.

The effect of the amplification of the waves is introduced assuming that the interfacial area, as expressed in equation (7), can be considered as a portion of the total surface of the bubble. For the definition of the area the surface should be expressed as arc integrals in three dimensions which is extremely complicated to be solved in a CFD code, therefore we treat it with the approximation to a square waves, so that the value of the wave amplified length is expressed simply as

$$L_{new} = L + \frac{kL\eta}{\pi} \quad (15)$$

$$L = \sqrt{a_i \Delta V} \quad (16)$$

where  $L$  is the square root of the interfacial area. The total area equals

$$S_{new} = \left( \frac{k\eta}{\pi} + 1 \right)^2 S_{square} \quad (17)$$

At this point the value of the wave number can be obtained as the one that maximizes the growth of the surface area, solving  $\frac{\partial^2 S_{new}}{\partial t \partial k} = 0$ . Such equation is transcendental and therefore it needs several approximations before reaching a solution that can be handled straight-forwardly by the CFD code. The solution can be obtained setting the derivative of eq. (14) to zero and neglecting the effect of the viscosity. In this case the equation is non-transcendental and reads

$$k_{max} = \sqrt{\frac{Ag(\rho_w + \rho_s)}{3\sigma}} \quad (18)$$

The acceleration can be calculated by the pressure gradient per unit volume which is trivial to obtain from a multi-purpose CFD code as STAR-CCM+. It is worth noting that we need only the pressure gradient across the surface or the region identified as the surface, so that in this region we need to obtain the vector normal to the surface pointing out the bubble and the applying the dot product as follows

$$g = \frac{\nabla P \cdot \frac{\nabla \alpha_w}{|\nabla \alpha_w|}}{\rho} \quad (19)$$

where  $\rho$  represents the average density of the fluid in the cell on the identified surface. The water volume fraction has been chosen for the definition of the normal vector so that the vector points out of the surface and in the same direction of the pressure gradient in case the pressure within the steam results lower than the surrounding value. The acceleration is considered effective for the RTI and the area amplification, only in case it assumes a positive value.

With the above considerations we have all the terms necessary to define at each iteration the expression of  $n$  in Eq. (14) and consequently the amplitude  $\eta$  in the current time step from the solution of eq. (1), is expressed in the code as:

$$\eta_t = \eta_{t-\Delta t} e^{n\Delta t} \quad (20)$$

where  $\eta_{t-\Delta t}$  represents the wave amplitude calculated at the previous time step in the code and is constant during each time step. Such possibility is obtained in STAR-CCM+ enabling the usage of the *sliding window* function [18]. At the first time step in the whole domain the amplitude is initialized as  $10^{-5}$  m. There is no particular evidence of the value to be employed for the initialization and a small number was chosen. The RTI problem is well known ill-posed problem where the initial conditions might affect the final results [17]. Sensitivity cases on the initial wave amplitude might be necessary in the future to verify the strength of the proposed model. A maximum value of the wave number have been set in each cell to maintain the amplitude small than the square root of the interfacial area in that cell as

$$\eta_t = \min\left(\eta_{t-\Delta t}, \sqrt{\nabla a_s \Delta V}\right) \quad (21)$$

where  $\eta_t$  is assumed the form of eq. (20). Finally the area density at the interface region is expressed in the code as:

$$a_{ij} = |\nabla \alpha_s| \left( \frac{k_{\max} \eta_t}{\pi} + 1 \right)^2 \quad (22)$$

### 3. EXPERIMENT VALIDATION AND MODEL

#### 3.1. STB-4 experiment

The main objective of the POOLEX project was to increase the understanding of condensation phenomena inside the wet well compartments of a BWR containment during steam discharge. Experimental results of the POOLEX project can be used for the validation of different numerical methods for simulating steam injection through a blow down pipe into liquid. The pool of the POOLEX facility is a cylinder shaped stainless steel pool open at the top. A sketch is presented in Figure 2.

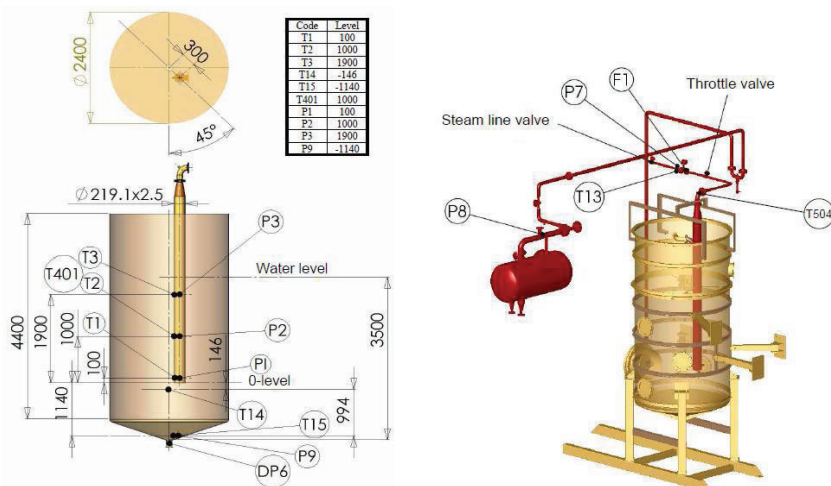


Figure 2 POOLEX facility sketch and isometric view [9].

The STB-28 experiment consisted of a long-running steam blowdown (duration 3195 s). The purpose of this test was to study the formation and condensation of steam bubbles at the blowdown pipe outlet as a function of pool water temperature. During the blowdown, seven short time intervals were recorded with

a high-speed camera (labeled from STB-28-1 to STB-28-7). The pool temperature rose from 47°C to 77°C during the test.

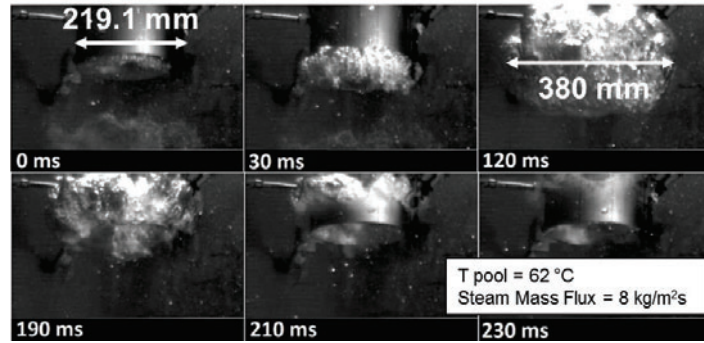


Figure 3 Images of chugging phenomenon in the STB-28-4 experiment [9].

Only the STB-28-4 experiment, characterized by a pool temperature of 62°C, is considered in this study. The steam mass flux remained at the level of 8.0 kg/m<sup>2</sup>s during the whole blowdown, equivalent to around 0.3 kg/s. The steam blowdown pipe is built in stainless steel with a diameter of 219.1 mm. The inflation and collapse of a bubble during the STB-28-4 blowdown is presented in Figure 3. The steam, going out from the pipe's mouth, forms a bubble which collapses and drags the pool water within the pipe, giving rise to the chugging phenomenon. In this experiment it is not possible to visualize the interface moving within the pipe so that experiments with polycarbonate pool and pipe are being performed at the SIET laboratories [14] and will be the subject of future numerical validation with the current approach.

### 3.2. STAR-CCM+ modeling

The domain was built without appealing to any approximation and respecting the asymmetries of the facility. A refined region was built close to the pipe outlet because large gradients are expected in this region (ref. to Figure 4 b).

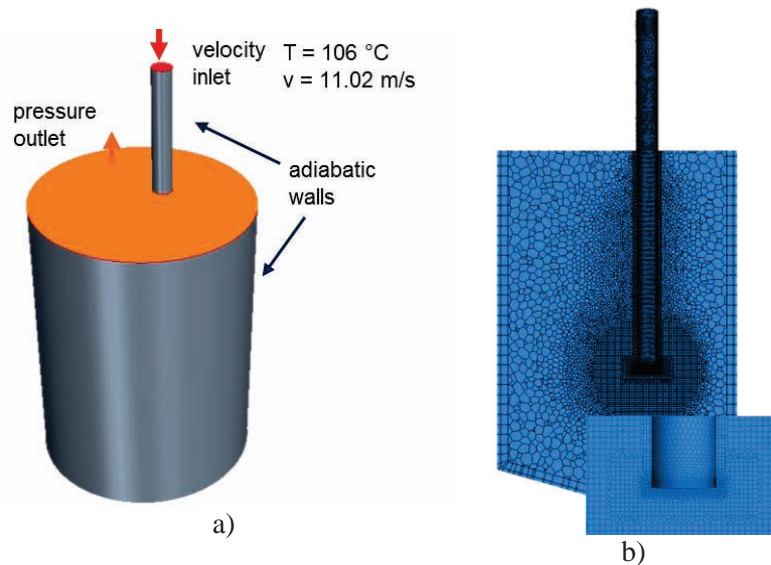


Figure 4 a) computational domain and b) discretization on a plane passing through the steam pipe.

The total mesh resulted in around polyhedral 500,000 elements. Steam velocity was imposed as inlet conditions of the pipe and steam assumed in saturated conditions while the pool water temperature was fixed at 62 °C (Figure 4 a).

The pipe, which is penetrating the pool, was not insulated in the experiment. In the approach developed in [9, 11] the steam condensation within the pipe, before discharge in the pool, was introduced by reducing the effective steam mass flow rate. This approach might be relevant in case we wished to consider a long transient and confirm the temperature distribution in the pool but is considered secondary for the study of a single bubble collapse, which is the case of the present analysis. The walls were therefore considered adiabatic and steam in saturated conditions.

### 3.2.1. Mesh sensitivity

The mesh sensitivity was performed on the discretization of the refinement on the sphere adopted at the pipe outlet. The absolute value of the polyhedral discretization is for the coarse, nominal and fine mesh equal to 0.025 mm, 0.02 mm and 0.015 mm respectively.

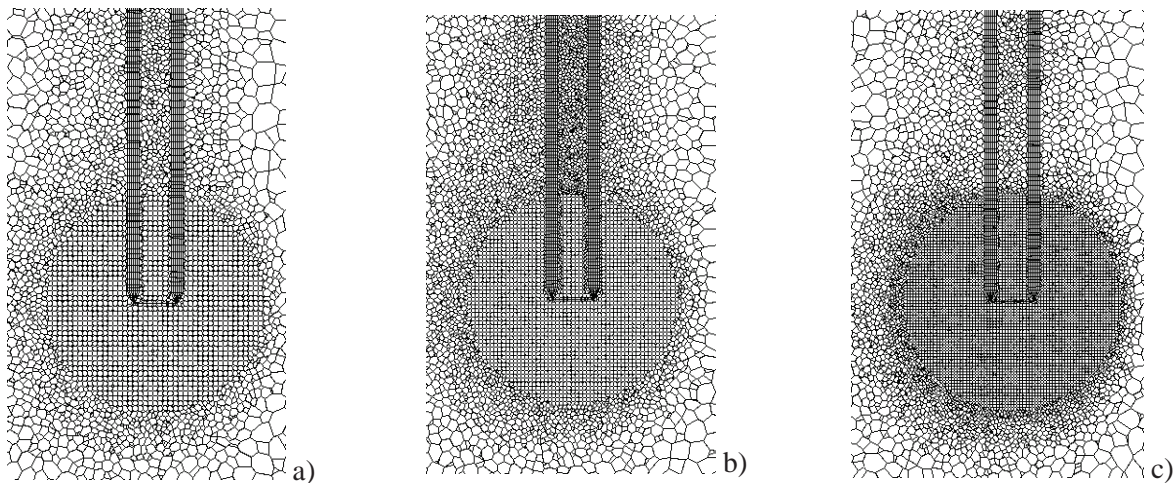


Figure 5 Grids employed for the mesh sensitivity. a) coarse, b) nominal and c) fine mesh.

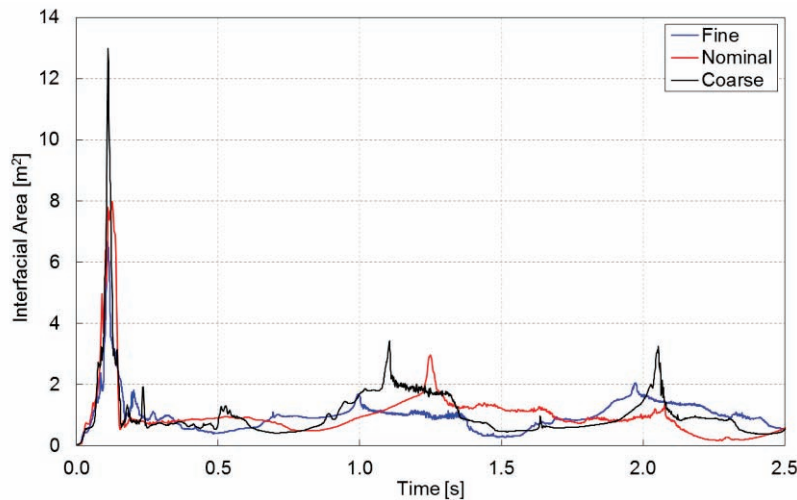
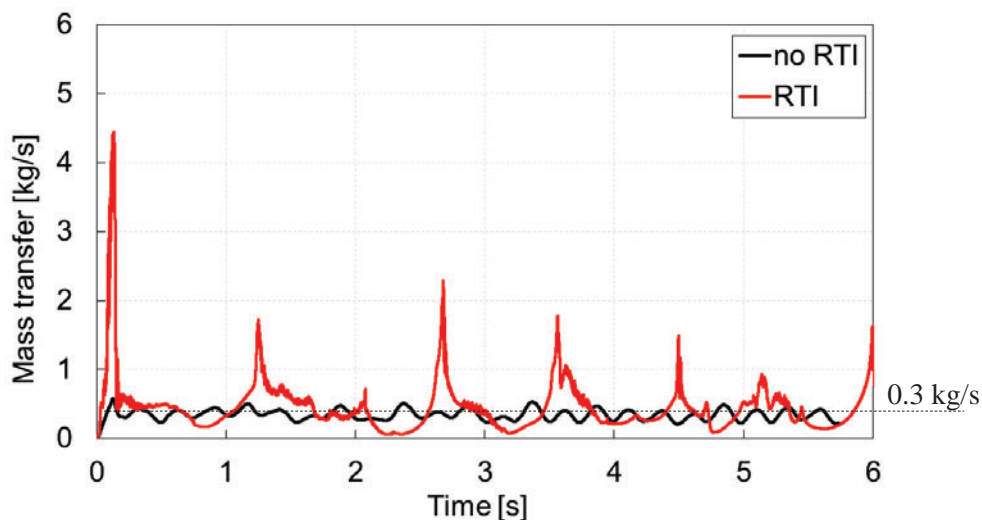


Figure 6 Interfacial area from the beginning of the simulation with each discretization mesh.

Figure 6 presents the interfacial area in the domain with the three grids reported above. From the macroscopic point of view of the chugging prediction there is not large difference among the three cases. The refinement has the effect to reduce the area peak at the bubble implosion. Also not large influence is visible in the prediction of the period among the cases with the interfacial area value varying less than 0.5 seconds. The coarse grid was not employed in the next calculations because its employment resulted in several large peaks of mass transfer later in the calculation, possibly denoting numerical errors due to the coarse discretization.

#### 4. RESULTS

The present results concentrate on several discharge cycles with the *nominal* mesh described in the previous chapter. The steam has been initialized 30 cm above the pipe mouth with the purpose to create a more physical temperature solution during the discharge period in the pool and avoid numerical errors. During the discharge in the pool the condensation mass transfer starts increasing for the combined effect of the increasing surface area, increasing water turbulence due to the steam jet and reduced subcooling determined by the large mixing. Figure 7 presents the comparison of the condensation mass transfer for the model adopting the minimum area (defined hereafter as *no RTI case*) and with the RTI. Figure 8 reports the volume fraction for the two cases. In the first bubble ejection the surface area is one order of magnitude larger compared to the *no RTI case*. Such large area increase is the result of the amplification do to the depressurization of the bubble. As depicted in Figure 8 only in the *RTI case* the steam reenters the pipe flowing upward, until the condensation mass transfer decreases below the mass flow rate provided at the inlet due to reduction of surface area and subcooling (Figure 7). At this point the flow starts moving downwards again with a new cycle of the phenomenon. In the present simulation around 10 cycles are computed.



**Figure 7** Computed results of a) condensation mass transfer and b) surface area. The value of the bubble equivalent diameter is calculated from the surface assuming a perfect sphere.

It is worth noting the different prediction of the frequency of the phenomenon that can be evaluated from the oscillating behavior of the mass transfer in Figure 7, which is proportional to the area growth associated to the bubble position outside the pipe mouth. In the *no RTI case* the frequency appears larger compared to the frequency calculated from the pressure signal in the experiment [11] which is around 0.1 Hz. The calculations including the RTI instead provide the frequency value in the same order of magnitude with what observed in the experiment. It is likely that the length of the pipe might play a role

in determining the frequency of the phenomenon but in this work we concentrate on qualitatively improving the results compared to largely differing predictions adopting usual models.

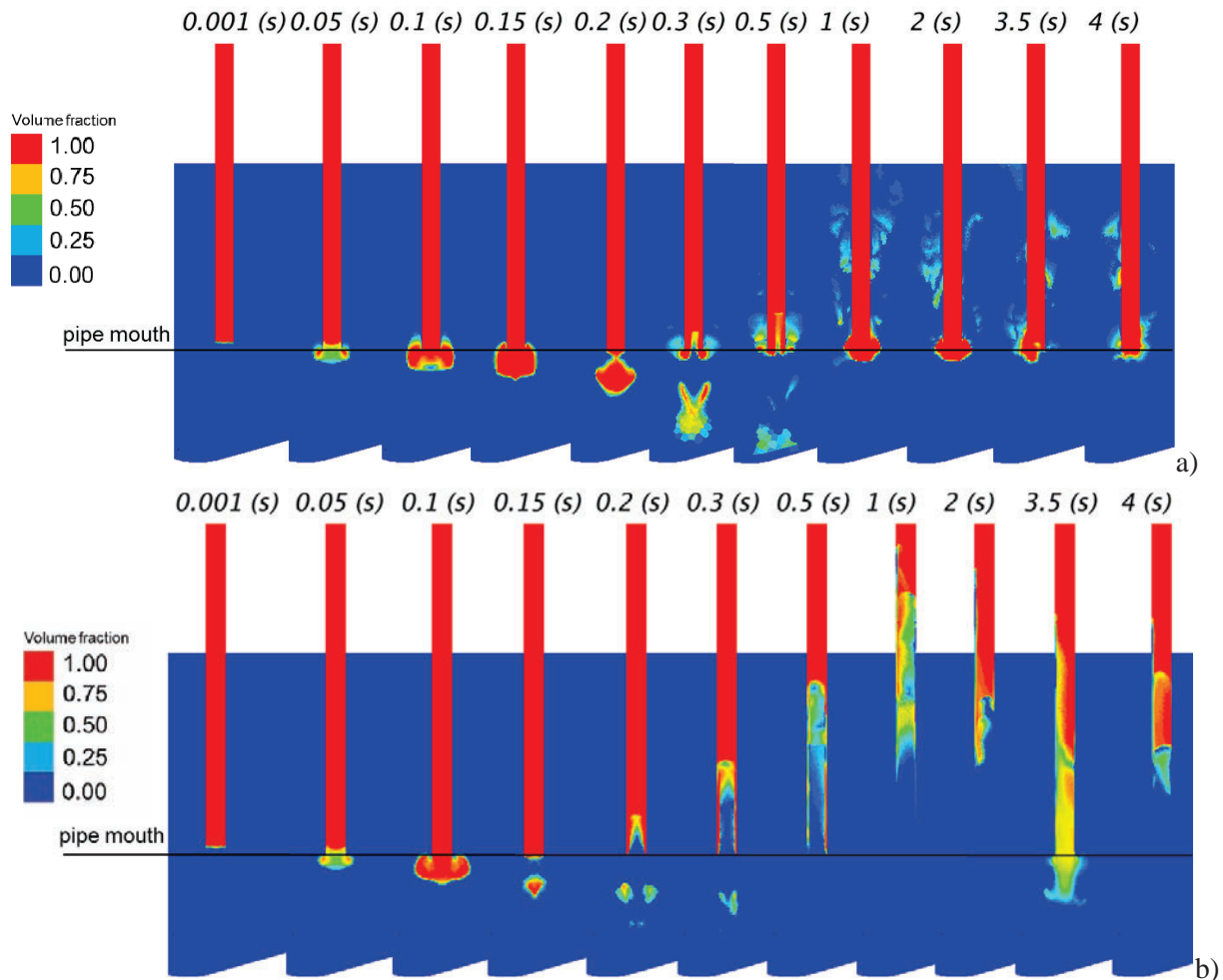
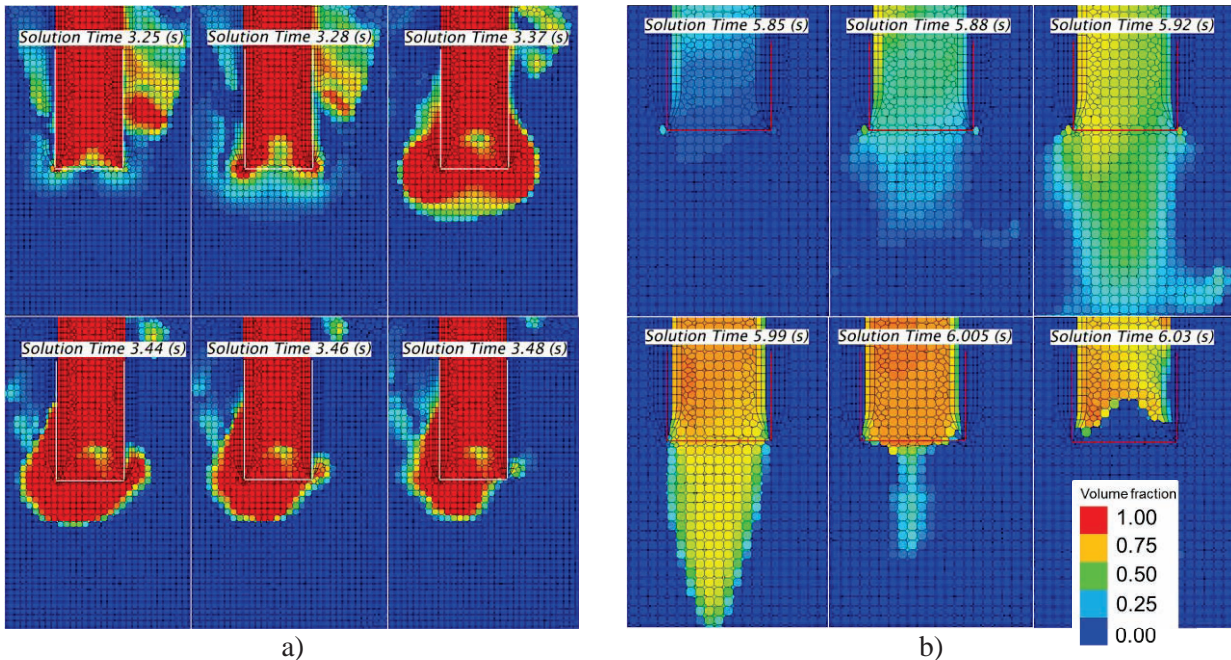


Figure 8 Volume fraction history, a) no RTI case, b) RTI case.

One bubble cycle is presented in Figure 9 a) and b) for the *no RTI case* and *RTI case*, respectively. In both cases images are selected in order to qualitatively compare with the experimental frames depicted in Figure 3 at the same relative time interval. In the no RTI case the bubble growth is similar to what observed experimentally (first 3 frames) but the bubble collapse is not predicted because turbulence itself is not responsible for such quick mass transfer. In Figure 9 b) the volume fraction at the pipe outlet does not reach the value of 1 but it reaches about 0.8. In general the two fluid model does not track the interface but the total area so that the result does not loses validity. In the case of RTI employment the last three frames agree in time well with the bubble collapse phenomenon and subsequent water interface moving within the pipe. The fact that the volume fraction is not close to one might be an indication that the Rayleigh-Taylor waves grow quicker compared to the reality. This can be imputed to the several approximations introduced above, such as the use of a square wave approximation, not accounting for wave canceling and not considering for the heat transfer variation between surfaces and troughs. Also the initialization of the wave amplitude might play some effect which could be tested through several sensitivity cases.



**Figure 9** Bubble implosion sequence predicted by STAR-CCM+. a) with the minimum surface area, b) with the introduction of RTI model for the surface area.

However the most remarkable difference among the computations is the ability to predict the surface moving within the pipe. In this direction the compressible model plays a critical role showing that after the first large bubble collapse the steam reduces the pressure to the extent to drag the steam back into the pipe. Also in the *no RTI* case some of the steam is transported to the top boundary due to incomplete condensation resulting from the computation of a too small area. In the experiment, even though a small window is visible, the steam appears condensing completely at this level of subcooling. With the introduction of the RTI model for the interfacial area, depicted in Figure 8 b) the steam condenses completely within the pool. In the perspective of the accident progression at any repetition of the new cycle a large amount of water with large momentum is discharged into the pool, thus affecting the water recirculation and mixing within the pool.

## 5. CONCLUSIONS

A novel model to account for steam-water surface instability in the case of steam DCC has been proposed and applied to a well-known condensation experiment. The present investigation contributes to an additional interpretation of the chugging phenomenon indicating the instability of the interfacial area as one of the main contributors during the bubble collapse. The instability and area amplification were described following the theory of the Rayleigh-Taylor instability and its implementation into a commercial multi-purpose CFD code (i.e. STAR-CCM+ 9.06.007) has been documented. The results present an improvement in the agreement with the experimental values compared to previous simulations that did not consider the area enhancement. It also proves an undoubted enhancement of the local phenomenological prediction during the bubble collapse. The validation is under current development for sensitivity of initial conditions (e.g. wave amplitude), turbulence and heat transfer models and in particular to demonstrate that the present method could be applied for different levels of subcooling and various sparger diameters (e.g. BWR pressure suppression pools).

## NOMENCLATURE

### Subscripts

$i, j$	phase $i, j$
$ij$	interface between phase $i$ and $j$
$w$	water
$s$	steam

### Variables

$Nu$	Nusselt number
$Re_t$	turbulent Reynolds number
$Pr$	Prandtl number
$u_t$	turbulent velocity scale
$l_t$	turbulent length scale
$k$	turbulent kinetic energy
$\varepsilon$	turbulent dissipation
$a_{ij}$	interfacial area density
$\eta$	wave amplitude
$n$	RTI function
$g$	gravity
$k$	wave number
$A$	Atwood number
$\nu = (v_w + v_s) / (\rho_w + \rho_s)$	kinematic viscosity

## REFERENCES

1. C.K. Chan, C.K.B. Lee, "A regime map for direct contact condensation," *Int. J. Multiphase Flow*, **8**(1), 11–20 (1982).
2. I. Aya, H. Nariyai, "Boundaries between regimes of pressure oscillation induced by steam condensation in pressure suppression containment," *Nucl. Eng. Des.*, **99**, pp. 31–40 (1987).
3. I. Aya, H. Nariyai, "Evaluation of heat-transfer coefficient at direct contact condensation of cold water and steam," *Nucl. Eng. Des.*, **131**, pp. 17–24 (1991).
4. K.S. Liang, P. Griffith, Experimental and analytical study of direct contact condensation of steam in water, *Nucl. Eng. Des.*, **147**, pp. 425–435 (1994).
5. S. Cho, C.H. Song, C.K. Park, S.K. Yang, M.K. Chung, "Experimental study on dynamic pressure pulse in direct contact condensation of steam jets discharging into subcooled water," *First Korea-Japan Symposium on Nuclear thermal Hydraulics and Safety*, Pusan, Korea, October 21-24, pp. 291-298, (1998).
6. A. Petrovic de With, R. K. Calay, G. de With, "Three-dimensional condensation regime diagram for direct contact condensation of steam injected into water", *Int. Journal of Heat and Mass Transfer*, **50**, pp. 1762-1770 (2007).
7. D.A. Sargis, J.H. Stuhmiller, S.S Wang, "A fundamental thermalhydraulic model to predict steam chugging phenomena", Proceedings of ASME 1978 Winter Meeting. Topics in Two-Phase Heat Transfer and Flow, pp.123-133 (1978).
8. H. Nariyai, I. Aya, "Fluid and pressure oscillations occurring at direct contact condensation of steam flow with cold water," *Nucl. Eng. Des.*, **95**, pp. 35-45 (1986).

9. V. Tanskanen, CFD modelling of direct contact condensation in suppression pools by applying condensation models of separated, Ph. D. Thesis, Lappeenranta University of Technology (2012).
10. Laine, J. and Puustinen, “Steam Blowdown Experiments on Chugging”, Research Report POOLEX 2/2005. Lappeenranta University of Technology, 2006.
11. V. Tanskanen, A. Jordan, M. Puustinen, R. Kyrki-Rajamäki, “CFD simulation and pattern recognition analysis of the chugging condensation regime”, *Annals of Nuclear Energy*, **66**, pp. 133–143 (2014)
12. E. D. Hughes, R. B. Duffey, “Direct contact condensation and momentum transfer in turbulent separated flows”, *International Journal of Multiphase flow*, **17**(5), pp. 599-619 (1991).
13. S. Banerjee, D. Lakehal, M. Fulgosi, “Surface Divergence Models for scalar exchange between Turbulent Streams,” *International Journal of Multiphase Flow*, **30**, pp. 963–977 (2004).
14. M. Pellegrini, L. Araneo, A. Achilli, H. Ninokata, M. Ricotti, M. Naitoh, “Suppression pool testing at the SIET laboratory: Experimental Investigation of Critical Phenomena Expected in the Fukushima Daiichi Suppression Chamber”, *Journal of Nuclear Science and Technology*, (2015) [*to be published*]
15. C. Josey, E. Baglietto, “Adding a Rayleigh-Taylor correction factor for the analysis of sparger operation”, MIT internal report, May 22, 2014
16. R.E. Duff, F.H. Harlow, C.W. Hirt, “Effects of diffusion on interface instability between gases,” *Physics of fluids*, **5**(4), pp. 417-425 (1962).
17. D. Livescu. “Compressibility effects on the Rayleigh-Taylor instability growth between immiscible fluids.” *Physics of Fluids* (1994-present), 16 (1): pp. 118–127
18. STAR-CCM+ 9.02.007, *User Manual*, (2014).
19. M. Ishii, T. Hibiki, “Thermo-fluid dynamics of two-phase flow”, Springer, Second Edition (2011).